RI 9567

REPORT OF INVESTIGATIONS/1995

In Situ Stress at the Lucky Friday Mine

(In Four Parts):

3. Reanalysis of Overcore Measurements From the Star Mine

UNITED STATES DEPARTMENT OF THE INTERIOR

UNITED STATES BUREAU OF MINES

U.S. Department of the Interior
Mission Statement

As the Nation's principal conservation agency, the Department of the Interior has responsibility for most of our nationally-owned public lands and natural resources. This includes fostering sound use of our land and water resources; protecting our fish, wildlife, and biological diversity; preserving the environmental and cultural values of our national parks and historical places; and providing for the enjoyment of life through outdoor recreation. The Department assesses our energy and mineral resources and works to ensure that their development is in the best interests of all our people by encouraging stewardship and citizen participation in their care. The Department also has a major responsibility for American Indian reservation communities and for people who live in island territories under U.S. administration.

Report of Investigations 9567

In Situ Stress at the Lucky Friday Mine

(In Four Parts):

3. Reanalysis of Overcore Measurements From the Star Mine

By J. K. Whyatt, M. J. Beus, and M. K. Larson

UNITED STATES DEPARTMENT OF THE INTERIOR
Bruce Babbitt, Secretary

BUREAU OF MINES
Rhea Lydia Graham, Director

International Standard Serial Number
ISSN 1066-5552

CONTENTS

ILLUSTRATIONS

TABLES

UNIT OF MEASURE ABBREVIATIONS USED IN THIS REPORT

Metric Units

cm	centimeter	m	meter
deg	degree	MPa	megapascal
GPa	gigapascal	pct	percent
kg/m^3	kilogram per cubic meter	με	microstrain
km	kilometer		

U.S. Customary Units

ft	foot	lb/ft^3	pound per cubic foot
in	inch	psi	pound per square inch

In Situ Stress at the Lucky Friday Mine

(In Four Parts):

3. Reanalysis of Overcore Measurements From the Star Mine

By J. K. Whyatt, M. J. Beus, and M, K. Larson

ABSTRACT

U.S. Bureau of Mines researchers reviewed an in situ stress estimate developed from measurements of overcore strain taken at test sites on the 7300 and 7500 levels of the Star Mine near Mullan, ID. Although the field measurements of overcoring strain were found to be useful, significant deficiencies were found in the stress estimation procedure. A new stress estimate was developed incorporating statistical methods and an improved understanding of stress concentration factors for interpreting overcore strains recorded by doorstopper cells. Spatial variability of overcore strains and the implications for stress field variability were explored.

---

[1]Mining engineer, Spokane Research Center, U.S. Bureau of Mines, Spokane, WA.

INTRODUCTION

Researchers from the U.S. Bureau of Mines (USBM) undertook the investigation described in this Report of Investigations (RI) to increase basic knowledge of the in situ stress field in the vicinity of the Lucky Friday Mine of the Coeur d'Alene Mining District of northern Idaho. The study is based on an overcore stress measurement reported by Beus and Chan (1980) as part of a USBM investigation into shaft design criteria for the Coeur d'Alene district. This stress measurement was chosen for reconsideration because the measurement site is conveniently located with respect to active USBM research projects at the Lucky Friday Mine (figure 1). Knowledge of the in situ stress field will provide important information for ongoing projects aimed at developing improved mining methods and mitigating rock-burst hazards at this mine. There was considerable potential for increasing the accuracy of the analysis by applying a least squares procedure and improved doorstopper cell stress concentration factors. Reanalysis of this stress estimate 15 years after the overcore measurements were taken and over 10 years after publication of a USBM RI describing the work (Beus and Chan, 1980) was made possible by the existence of good, detailed records maintained in USBM research files.

Previous reports in this series [Whyatt and Beus, 1995 (part 1); Whyatt and others, 1995a (part 2)] analyzed overcore stress measurements conducted on the 4250 and 5300 levels of the Lucky Friday Mine. A fourth and final report presents observational evidence of stress field orientation (Whyatt and others, 1995b). The final report also characterizes the stress field in the vicinity of the Lucky Friday Mine.

REVIEW OF AVAILABLE INFORMATION

The Star Mine stress measurement was originally pursued to develop an estimate of the natural in situ stress field in the vicinity of the mine. A good estimate of the natural stress condition required that the overcore measurement site be located far enough from mining to avoid mining-induced stress. On the other hand, cost considerations required that the site lie within mine development openings. Furthermore, a site with competent rock was sought to ensure that sufficient core recovery could be obtained for a successful measurement.

The stress field reported by Beus and Chan (1980) was based on 30 doorstopper cell overcore measurements in 3 boreholes at a site located on the east end of the 7300 level (figure 2). These measurements were taken between July and October 1975. In April and May 1975, six doorstopper cell overcore measurements were taken in a single borehole on the 7500 level 350 m (1,150 ft) to the west of the 7300-level site. The 7500-level measurements were not included in the original analysis.

The 7300-level site lies in rocks of the Revett Formation near the intersection of the Morning East and Grouse veins. The Revett Formation is part of the Belt Supergroup and consists of (1) sericitic quartzite beds that range in thickness from 15 to 61 cm (6 in to 2 ft) and (2) thin interbeds of argillite generally less than 2.5 cm (1 in) thick. Variations in sericite produce rocks with a considerable range of stiffness, strength, and brittleness. The quartzite beds also contain a small-scale depositional fabric, which has been shown to be associated with strength and deformational anisotropy at some locations within the district (Whyatt, 1986).

Bedding at the 7300-level site is nearly vertical, and some beds are overturned. Strike of the beds varies across the Morning East vein. There is a significant change in lithology as well. Rock south of the Morning East vein is a relatively stiff quartzite, while rock to the northeast of the vein is a relatively soft sericitic quartzite.

The 7500-level site lies on the north side of the Morning East vein but south of the Main vein and toward the middle of the mine. It also lies in the Revett Formation. Bedding dips steeply and strikes to the north and slightly west.

EXPLORATORY BOREHOLES AND PHYSICAL PROPERTY TESTS

The important role of geology at the site was recognized at the outset by the investigators. EX-size boreholes were drilled parallel, perpendicular, and diagonal to bedding about 30 cm (12 in) below the planned BX-size overcore boreholes. A borescope survey of the EX boreholes was used to map fractures and identify depths at which in situ modulus measurements would have the best chance of success (figure 3).

The in situ modulus tests (table 1) were conducted with a Colorado School of Mines (CSM) dilatometer (Hustrulid, 1971) in November 1975. The four basic components of this device are a polymeric cell (packer) that fits an EX borehole, a water-based fluid, a hydraulic pump, and a pressure gauge. The packer is inflated inside the borehole by hand cranking a screw-type pump that displaces a measured amount of fluid with each crank. Deformation of the borehole is reflected by

Figure 1

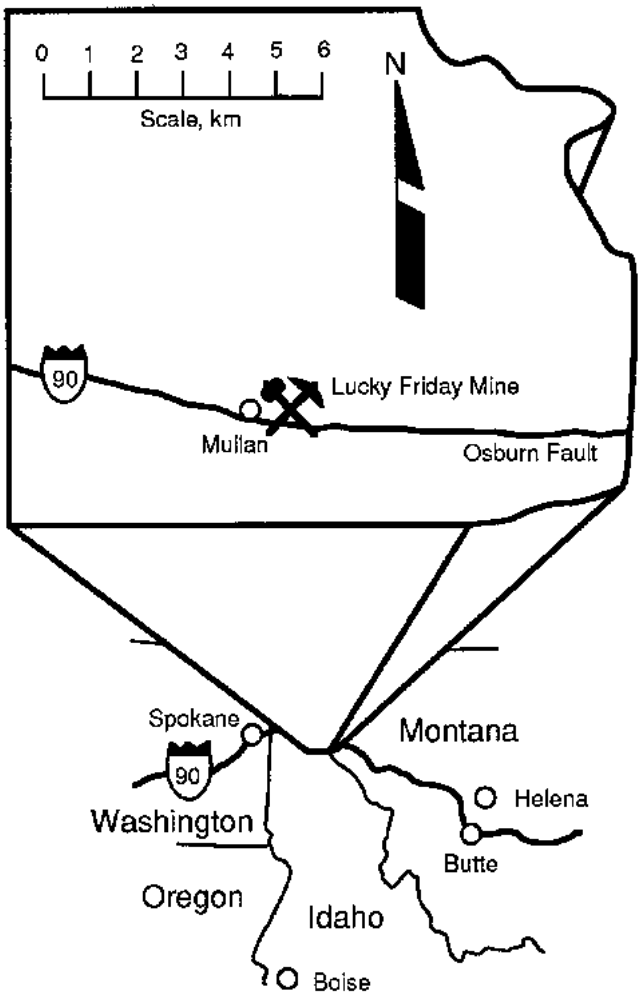

Location of Star and Lucky Friday Mines in Coeur d'Alene Mining District of northern Idaho.

the amount of fluid pumped into the packer. The modulus of deformation is obtained by comparing pressure and volume field records with records from laboratory tests on known materials.

The dilatometer tests found marked anisotropy of in situ modulus with bedding (Patricio and Beus, 1976), with results reproducible to within ±2 pct. However, the dilatometer is calibrated to estimate the elastic modulus of an isotropic material. That is, the inflation of the packer is assumed to proceed uniformly around the circumference of the borehole. If rock stiffness is anisotropic, expansion of the borehole will be greater in some directions than in others.

Table 1.—In situ modulus as measured by CSM dilatometer

Bore-hole	Borehole angle to bedding	Number of test locations	Mean modulus of deformation		Standard deviation	
			GPa	10^6 psi	GPa	10^6 psi
E1	0°	3	48	7.0	19	2.7
E2	90°	3	77	11.1	19	2.7
E3	45°	12	68	9.8	25	3.6

Amadei and Savage (1991) provide the anisotropic solution for the dilatometer, but require measuring diameter deformation in a number of directions as provided by modern versions of the dilatometer. Thus, their solution cannot be applied to estimating orthotropic properties from available CSM dilatometer information. Volume change will approximately reflect the average change in borehole radius. This is not a problem where a borehole is perpendicular to bedding because of the symmetry perpendicular to the borehole. At other orientations, however, resistance to change of radius in the stiff direction dilutes the impact of the soft direction, producing an intermediate estimate of elastic modulus. Thus, the in situ modulus measurements shown in table 1 likely understate the degree of anisotropy. Beus and Chan (1980) acknowledged this apparent anisotropy but did not pursue it further in laboratory testing or integrate it into their in situ stress estimates. The large standard deviations for the in situ measurements considerably exceeded the expected ±2 pct variation. The extra variability reflected changing rock properties with position in the borehole.

Laboratory tests on the EX core samples from borehole 1 only were used to determine the average elastic modulus of 63.8 GPa (9.26 million psi) reported for the site by Beus and Chan (1980). The orientation of bedding or structure in these samples was not recorded, but at the collar, bedding paralleled the borehole. The in situ modulus measured in borehole E2, which loaded the rock approximately parallel to bedding, exceeded the laboratory value for cores from borehole E1, which were also loaded parallel to bedding. In situ values of modulus were generally lower than laboratory values because of the larger volume of rock tested and because flaws were included that broke core samples during drilling. The source of this discrepancy is not evident but may arise from differences in the rocks tested. Cores from borehole E1 sampled a very limited thickness of strata that lay on top of the strata drilled in borehole E2. Unfortunately, further information on the type of rock involved in these tests was not available.

Figure 2

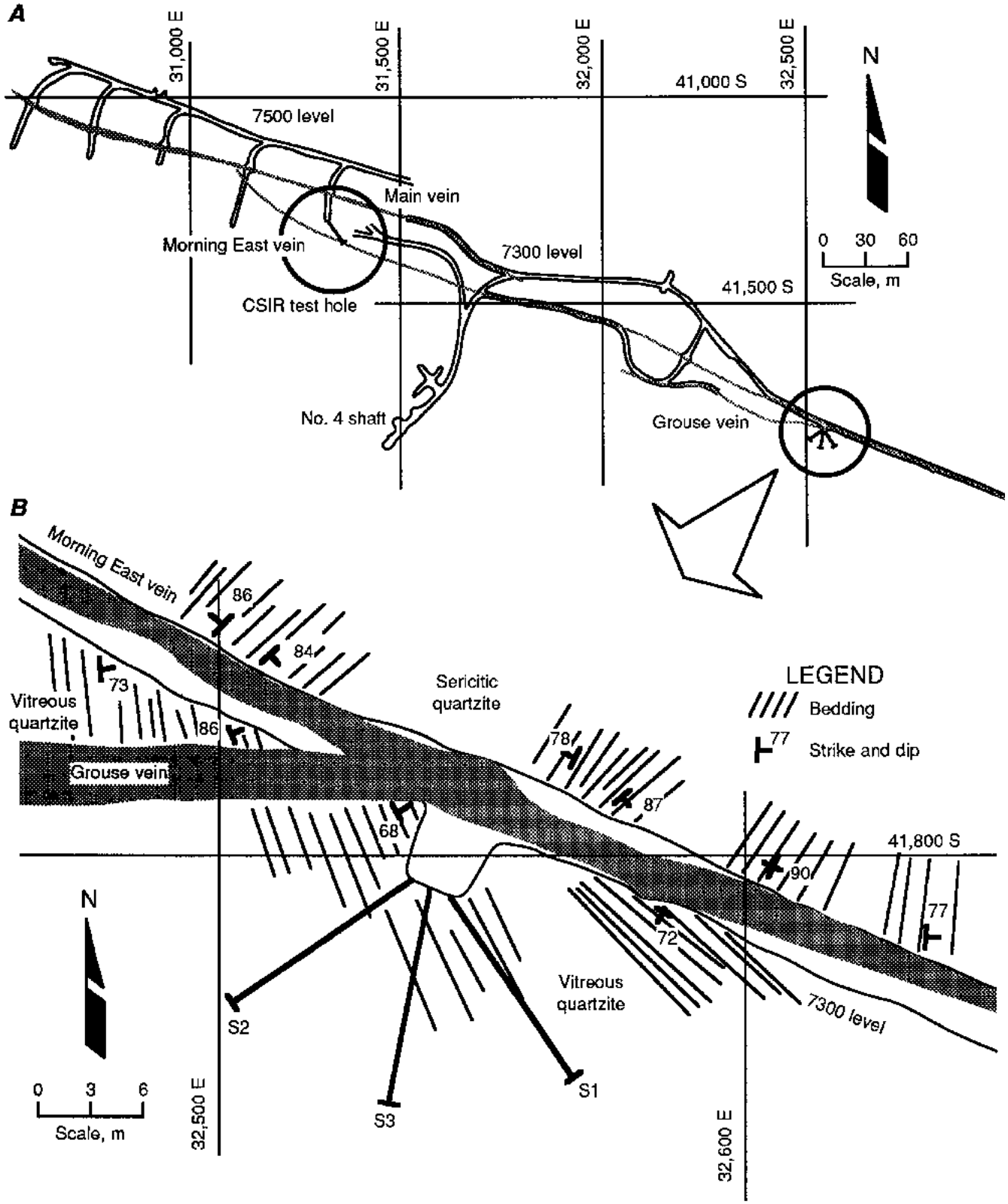

Location of 7300- and 7500-level test sites (A) with detail of 7300-level site (B).

Figure 3

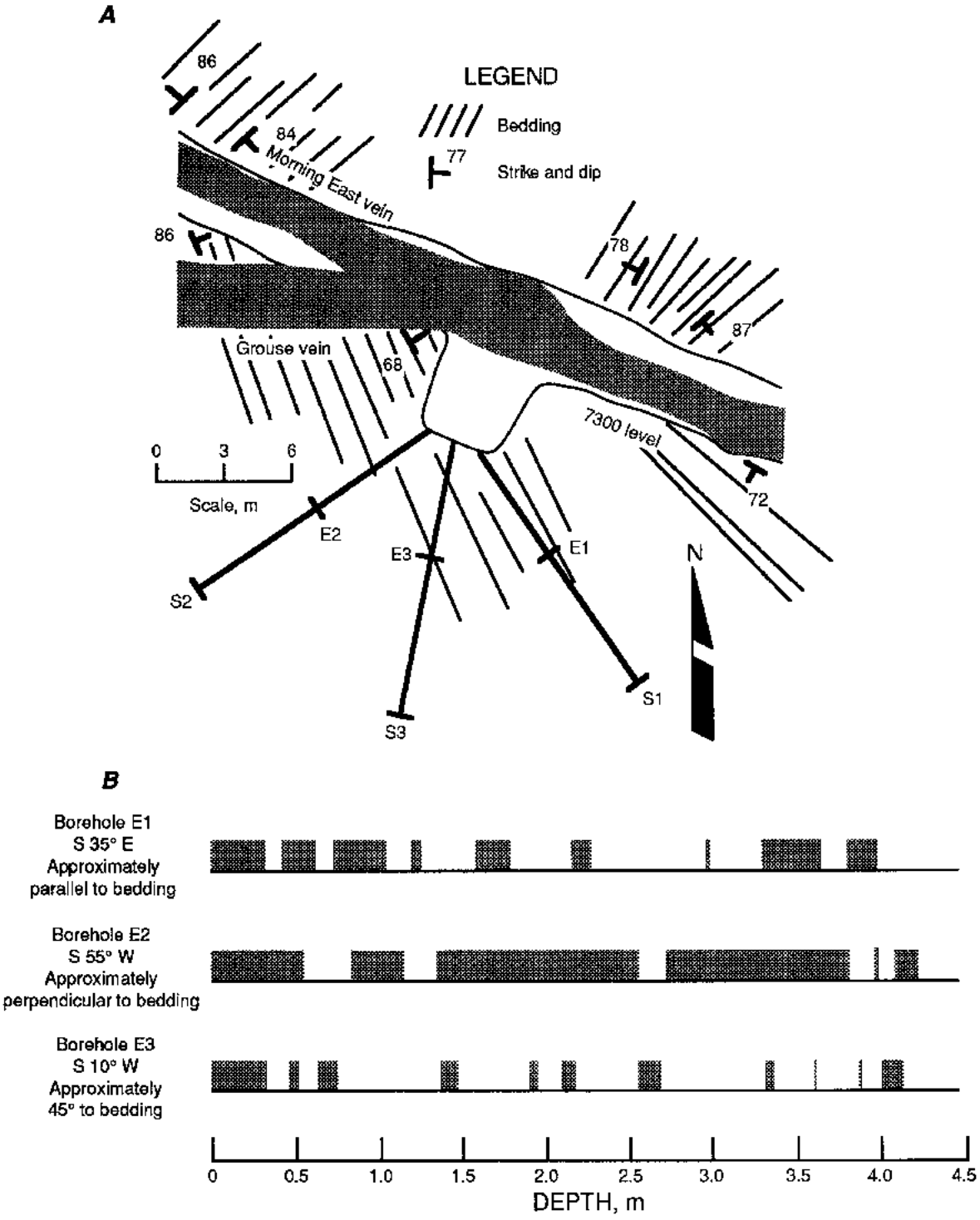

Borescope maps. A, Map of 7300-level site showing fracture-mapping boreholes (E1 to E3) and overcoring boreholes (S1 to S3); B, fractured rock core (shaded portions) for boreholes E1 to E3.

OVERCORE PROCEDURE

The Council for Scientific and Industrial Research (CSIR) biaxial strain cell, commonly known as a doorstopper, was selected for the overcore strain measurements. The doorstopper cell uses a four-element strain gauge rosette (figure 4) to measure strain release as a diamond drill passes (overcores) the cell. The difficulty of obtaining good core recovery at the site made the doorstopper cell a particularly good choice. The doorstopper cell requires only about 8 cm (3 in) of 6-cm (2.375-in) diam core for a successful measurement (Jenkins and McKibbin, 1986), while alternative types of cells require longer and larger diameter cores.

Although the doorstopper cell was not included in International Society for Rock Mechanics (ISRM) standard test procedures for overcore stress measurements (ISRM, 1987), the procedure described was generally consistent with guidelines for overcoring similar instruments and the manufacturer's recommended procedure. An installation tool helps with the task of centering and orienting the doorstopper cell, which is glued to the polished end of the borehole to measure distortion as the borehole is drilled. Load on the end of the rock core is relieved where the cell is glued. The installation tool houses a second doorstopper cell glued to a similar piece of core to compensate for changes in temperature.

The doorstopper cell glue is allowed to set up overnight, after which a series of readings is taken to establish baseline strain. The installation tool and wiring are then removed for overcoring. The doorstopper cell is small enough that properly centered cells are not affected by extending the diamond-drilled borehole (overcoring) to release stress on the face of the core. After overcoring, the installation tool is reattached to the doorstopper cell and a number of final readings are taken.

Determination of a full three-dimensional in situ stress state requires data from doorstopper cells in three boreholes. However, the gauges are fairly inexpensive, so installing several cells in each borehole is economically feasible.

Overcoring procedures have changed somewhat since this measurement was completed. The changes have improved the likelihood that a doorstopper cell installation will be successful, but have not changed the accuracy or validity of a successful overcore. This review of overcoring procedure and field notes encouraged confidence in the quality of the field measurements.

DATA-REDUCTION PROCEDURE

The procedure used by Beus and Chan (1980) to develop the reported Star Mine stress field estimate was typical of early Coeur d'Alene district investigations that have been found to suffer from a number of shortcomings (Whyatt and Beus, 1995). The application of this procedure to the Star Mine overcore measurements is traced through the remainder of this section.

Evaluate measurement quality.

The first step in the original procedure was to filter unreliable measurements. About half of the strain readings survived this step. Notes for discarded measurements attributed failure to a number of problems, including difficulties with gluing the gauges to the end of the borehole, water fouling the gauges, and lapses in overcoring procedure. Although data were collected for one borehole at the 7500-level site and three boreholes at the 7300-level site, only the 7300-level site was fully analyzed and reported by Beus and Chan (1980).

The measurements deemed to be reliable are underlined in table 2, which includes some notes about the specific difficulties encountered during overcoring.

Develop strain estimates for each gauge orientation.

The best overcore strains (underlining in table 2) were averaged to obtain the set of 12 composite overcore strains shown in table 3 (one for each gauge orientation in each borehole).

Collect strain components in a convenient coordinate system.

Eight of the composite overcore strains that happened to lie in a convenient coordinate system were selected and the rest were dismissed. That is, data selected in the previous step from –45° gauges in all boreholes and from +45° gauges in one borehole were excluded from the stress solution. The vertical overcore strains from each borehole were combined into a single average vertical overcoring strain measurement to reduce the set further, resulting in the six overcore strain measurements presented in table 4. This rather arbitrary elimination of data appeared to be mandated by a stress solution program requirement that strain components must lie conveniently in a local Cartesian coordinate system and that the solution be exactly determined. The coordinate system was defined by the two outer and roughly horizontal boreholes, which represented the x and y axes, and an upward z axis.

Figure 4

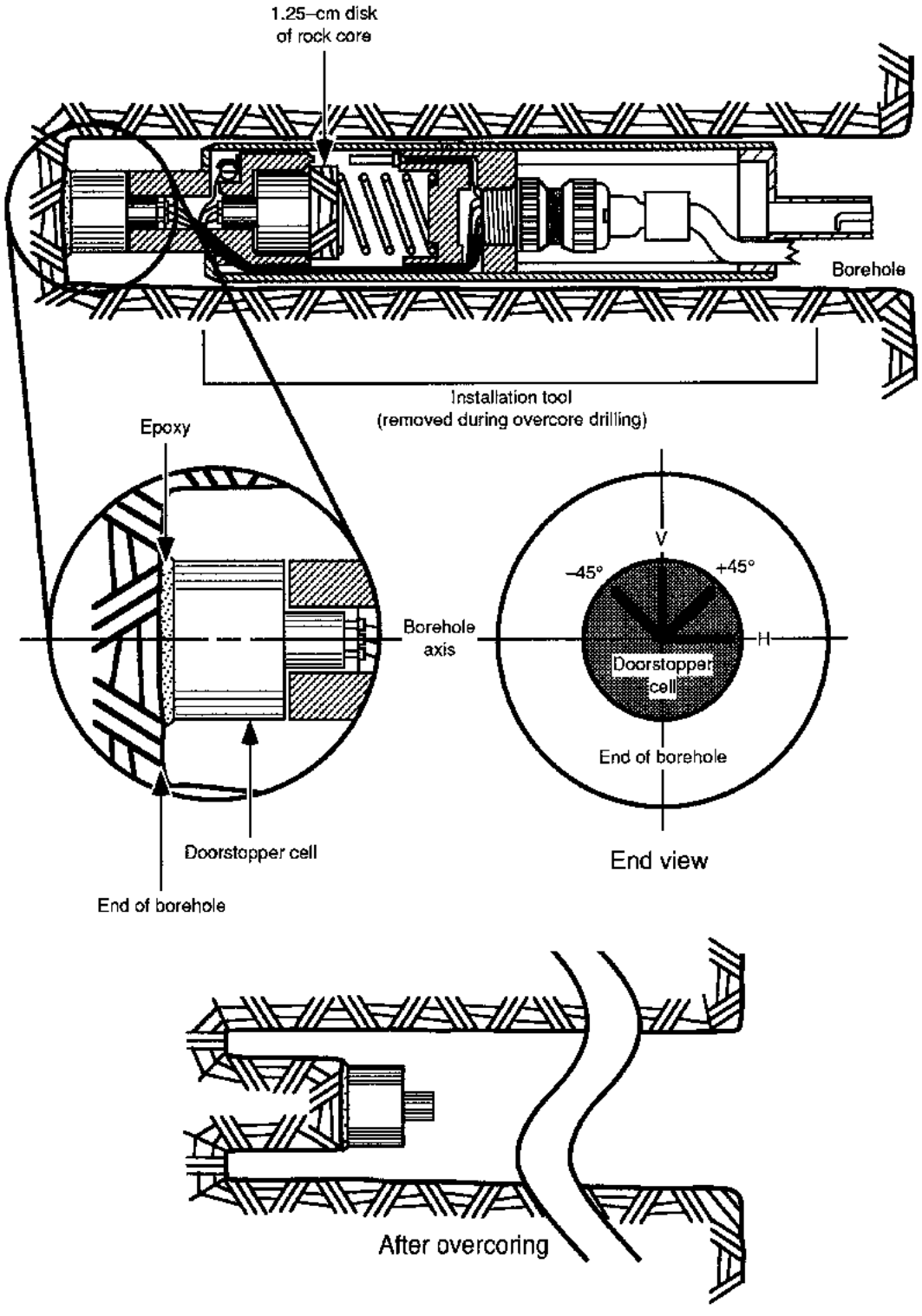

Schematic of CSIR doorstopper cell in borehole. (H = horizontal; V = vertical.)

Table 2.—Summary of strain data from doorstopper cell overcoring at Star Mine

Doorstopper cell	Strain by gauge orientation, με				Borehole depth, m	Notes
	+45°	-45°	Vertical	Horizontal		
7300-LEVEL SITE						
Borehole S1, oriented S 35° W, 5.5°:						
1	577	-28	619	-59	1.2	Induced stress zone.
2	363	133	521	-42	1.3	Bad glue joint.
3	39	-230	-27	-100	1.7	Induced stress zone, bad glue joint, bad surface preparation.
4	24	267	492	-212	7.2	
5	275	704	629	205	7.4	Conglomerate marker bed.
6	46	-78	-7	-55	7.7	Problem with reading gauges.
7	320	283	210	355	7.9	Crack at center of face.
8	471	29	312	135	8.4	
9	-69	-113	-251	26	11.5	Bad glue joint.
10	525	455	257	515	11.8	Poor bond, fracture along core.
Borehole S2, oriented S 55° W, 3.5°:						
1	456	869	325	890	4.0	
2	665	530	498	645	5.4	
3	741	338	43	962	6.0	
4	138	37	-132	282	9.1	
5	-15	379	112	256	9.4	
6	120	284	118	390	9.7	
7	114	1,153	207	968	10.2	
9	72	315	-105	452	11.0	
11	40	131	-91	392	11.8	Poor bond.
12	57	527	66	459	11.9	
13	-11	-40	-24	-15	12.2	Poor bond.
14	68	-36	-125	228	12.6	
Borehole S3, oriented S 10° W, 5.5°:						
1	206	19	96	221	3.4	
2	567	185	204	530	3.7	
3	573	180	224	476	4.0	
4	500	141	395	202	4.3	
5	209	27	147	83	4.7	
6	195	147	-36	390	5.0	Microfractured core face.
7	382	318	336	322	5.3	
9	472	534	533	409	11.8	
7500-LEVEL SITE						
Borehole 1, oriented S 40° E, 8°:						
1	432	1,890	639	-161	2.9	
2	442	116	371	159	3.1	
3	687	408	500	467	5.9	
4	217	-328	178	-46	6.1	Poor bond, fracture along core.
5	56	-28	123	-105	8.2	Poor bond, water on surface.
7	352	44	301	46	8.7	Core broke up.

NOTE.—Underlining indicates that these strain readings were used in calculating mean strains shown in table 3.

Table 3.—Average strain readings

Number of samples	Strain gauge orientation	Mean, με	Standard deviation
Borehole S1; doorstopper cells 5, 7, 8, 10:			
4	Horizontal	303	169
4	+45°	398	119
4	Vertical	352	189
4	-45°	368	284
Borehole S2; doorstopper cells 1, 2, 3, 7, 12:			
5	Horizontal	785	225
5	+45°	407	312
5	Vertical	228	189
5	-45°	683	325
Borehole S3; doorstopper cells 2, 3, 4, 7, 9:			
5	Horizontal	388	130
5	+45°	499	78
5	Vertical	338	134
5	-45°	272	161

Table 4.—Selection and interpretation of strain measurements

Borehole	Strain gauge orientation	Average, με	Assumed strain component
S1	Horizontal	303	ϵ_x
S2	Horizontal	785	ϵ_y
S1, S2, S3	Vertical	306	ϵ_z
S3	Horizontal	388	$^1\gamma_{xy}$
S2	+45°	407	$^1\gamma_{yz}$
S1	+45°	398	$^1\gamma_{xz}$

[1]This is an incorrect definition of shear strain.

Unfortunately, the last three composite strains in table 4 were interpreted as shear strains instead of normal strains in a direction diagonal to the coordinate axes. In other words, the +45° strain gauge data from the doorstopper cell were taken as shear strain on the face of the borehole. In fact, the shear strain arises from normal strains according to the relationship

$$\gamma_{PR} = 2\epsilon_Q - \epsilon_P - \epsilon_R, \quad (1)$$

where γ_{PR} = shear strain on borehole face,

and ϵ = normal strain measured by strain gauges in various orientations (shown in figure 5).

A complete development of strain components from a 45°-strain gauge rosette like that used by a doorstopper cell can be found in most texts on experimental stress analysis (e.g., Dalley and Riley, 1978). This error was sufficient to invalidate the reported strain field, and, as carried through the next two steps, to invalidate the stress field estimate.

Calculate three-dimensional strain tensor.

The strain tensor follows exactly from a set of six independent strain components. These results were invalidated by the incorrect definition of shear strain, as noted in the previous step.

Calculate three-dimensional stress tensor.

The strain tensor (table 4) was converted to the stress tensor using Hooke's law and adjusted for the stress concentration effect at the end of the borehole. Elastic properties for the stress estimate were determined by laboratory tests on core samples. Beus and Chan (1980) report material properties of Young's modulus = 63.8 GPa (9.26 million psi) and Poisson's ratio = 0.29.

The modern description of the relationship between in situ stress and concentrated stress at the end of a borehole is given by equations 2 through 4 (Rahn, 1984).

$$s_{xx} = a\sigma_{xx} + b\sigma_{yy} + c\sigma_{zz}, \quad (2)$$

$$s_{yy} = b\sigma_{xx} + a\sigma_{yy} + c\sigma_{zz}, \quad (3)$$

and $$s_{xy} = (a - b)\sigma_{xy} = d\sigma_{xy}, \quad (4)$$

where s = stress on end of borehole,

a, b, c, and d = constants,

σ = in situ stress field components,

and x, y, and z = coordinate axes.

Figure 5

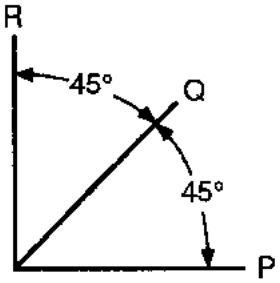

Normal strain orientations used in equation 1.

The constants a, b, c, and d link the in situ stress field components (σ) with the stress components on the end of the borehole(s). The solution procedure originally followed used borehole stress concentration factors of a = d = 1.25 and b = c =

0, attributed to an unpublished finite-element analysis by Chan and Beus.[2]

The theoretical basis for estimating the in situ stress field from doorstopper cell strain measurements has evolved considerably since introduction of the cell, and a number of sets of constants have been proposed since Beus and Chan (1980) reported this measurement. The variations in stress field estimates that result from the various sets of constants are examined in appendix A.

The resulting stress field estimate is presented in table 5. Although the estimate suffers from misdefinition of shear strain, it still provides a reasonable direction for the maximum principal stress and is reasonably close to the estimated overburden stress of 60 MPa (8,670 psi) for the site estimated by Beus and Chan (1980).

Table 5.—In situ stress field at 7300-level site as calculated using principal stress

Stress component	Magnitude		Bearing	Plunge
	GPa	psi		
σ_1	76	11,000	S 12° E	28°
σ_2	51	7,400	N 84° W	33°
σ_3	42	6,100	N 54° E	45°
σ_{h1}	67	9,700	N 21° W	
σ_{h2}	50	7,200	S 69° W	
σ_v	53	7,700		

NOTE.—Empty cells in columns intentionally left blank.

NOTE.—Principal stresses are presented as reported by Beus and Chan (1980), except for secondary horizontal (σ_{h1}, σ_{h2}) and vertical (σ_v) principal stress components, which are corrected values reported by Whyatt (1986).

STRESS FIELD ESTIMATE

An accurate estimate of the in situ stress field relies on determining which of the many overcore strain measurements were reliable and then applying statistical procedures and accurate stress concentration factors to minimize estimate error. Ideally, the mine rock mass would be homogeneous and isotropic and would not be influenced by mining. In this case, the estimate would accurately represent the natural stress field that is loading mine openings.

Stress estimates were calculated from strain data using the computer program STRESsOUT (Larson, 1992). STRESsOUT uses a standard set of assumptions to develop estimates of in situ stress from overcore strain measurements by minimizing the squared error for each strain measurement. By treating all measurements throughout the test site equally, it is assumed that (1) stress and material properties at a site are homogeneous and (2) the rock mass is linearly elastic and has no discontinuities. The program is capable of providing statistical treatment of the data[3] and improved adjustments for the induced stress field on the borehole.[4]

EVALUATION OF STRAIN DATA

The evaluation of strain data, especially the identification of invalid measurements, is a critical step in estimating the in situ stress field. Field notes describing difficulties with the instruments, bad glue joints, or rock defects are the most important source of information (table 2). Further insight can be gained by applying a number of screens that numerically test the overcore strains against various criteria.

A simple screen consists of solving for the stress field (S_1 and S_2)[5] measured by each of the various sets of three strain gauges at each doorstopper cell and comparing the results. A sound doorstopper cell overcore measurement should produce substantially the same stress field regardless of which gauges are chosen. Local solutions for the overcore strains in table 2 are developed in appendix B and illustrated in figure 6. The relative quality of each solution is ranked by assigning it to one of five arbitrarily defined groups (table 6). Definition of these groups followed criteria that proved to be useful in analyzing overcore measurements from the 5300 level of the Lucky Friday Mine in part 2 (Whyatt and others, 1995a) of this series of reports.

A related screen checks the self-consistency of a doorstopper cell by determining whether all four gauges of a cell are measuring the same strain field. This "strain

[2] Chan, S. S. M., and M. J. Beus. Determination of Three-Dimensional Stress in Brittle Rocks of Deep Mines With Biaxial-Strain Cells. Paper 2666 presented at Spring Meeting of the Society for Experimental Stress Analysis, Dallas, TX, May 15-20, 1977, 17 pp.

[3] A least squares routine ensures equal (or specified) weighting of all data points. This program runs on 8088 or better DOS-based personal computers in a matter of minutes, providing the capability to conduct parametric studies if needed.

[4] Advanced modeling techniques have led to development of more exact stress concentration factors that include the effect of Poisson's ratio. The program uses stress concentration factors specified by the user.

[5] S_1 and S_2 are nonstandard notations for the principal stress components on the end of a borehole (standard notations are σ_1 and σ_2). These nonstandard notations are needed to emphasize that they are not far-field in situ stress components.

Figure 6

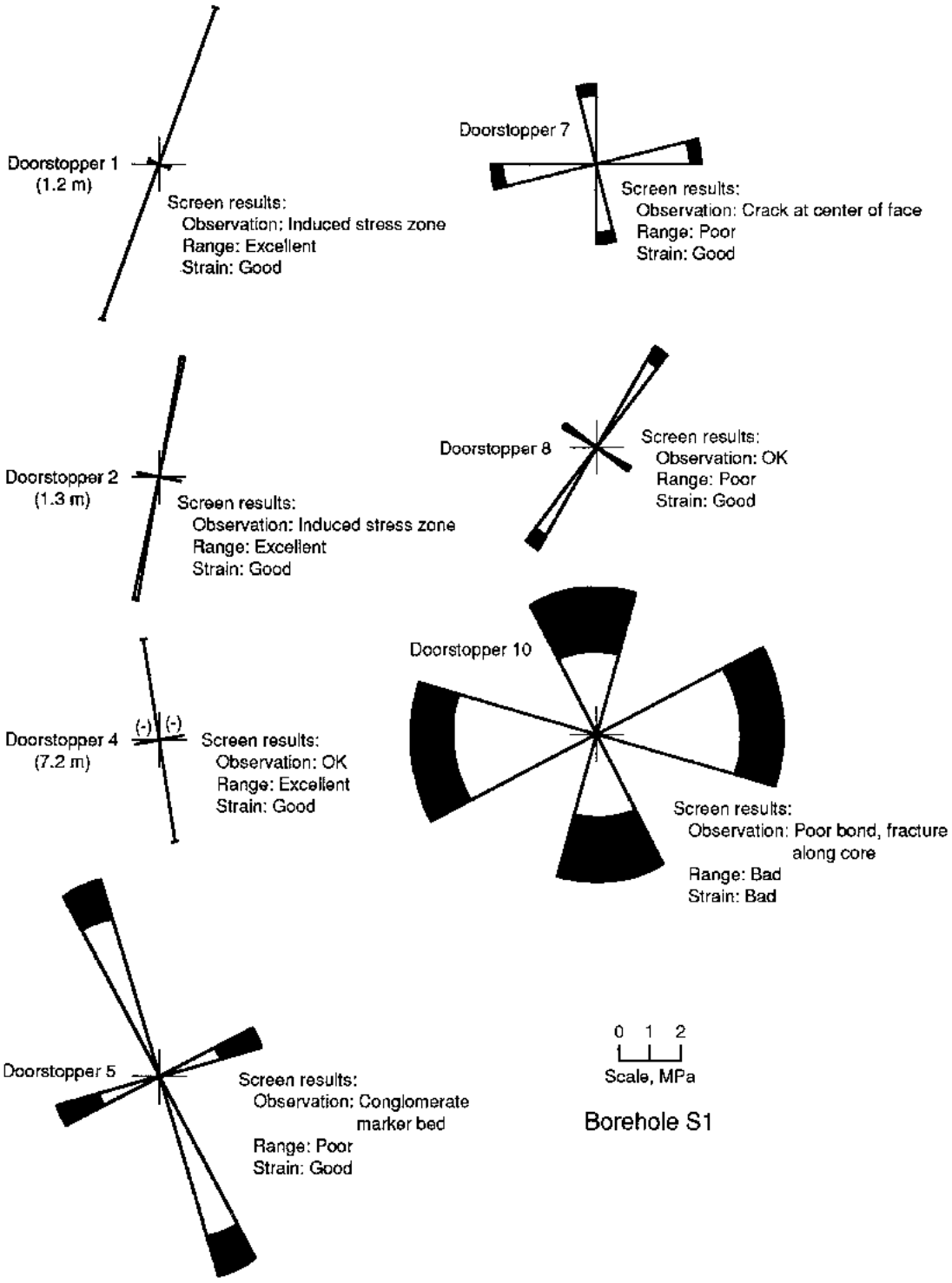

Range of stress fields measured on end of borehole by various sets of strain gauges in each doorstopper cell (see appendix B for calculations). Observations and results of range and strain screens are noted.

Figure 6—Continued

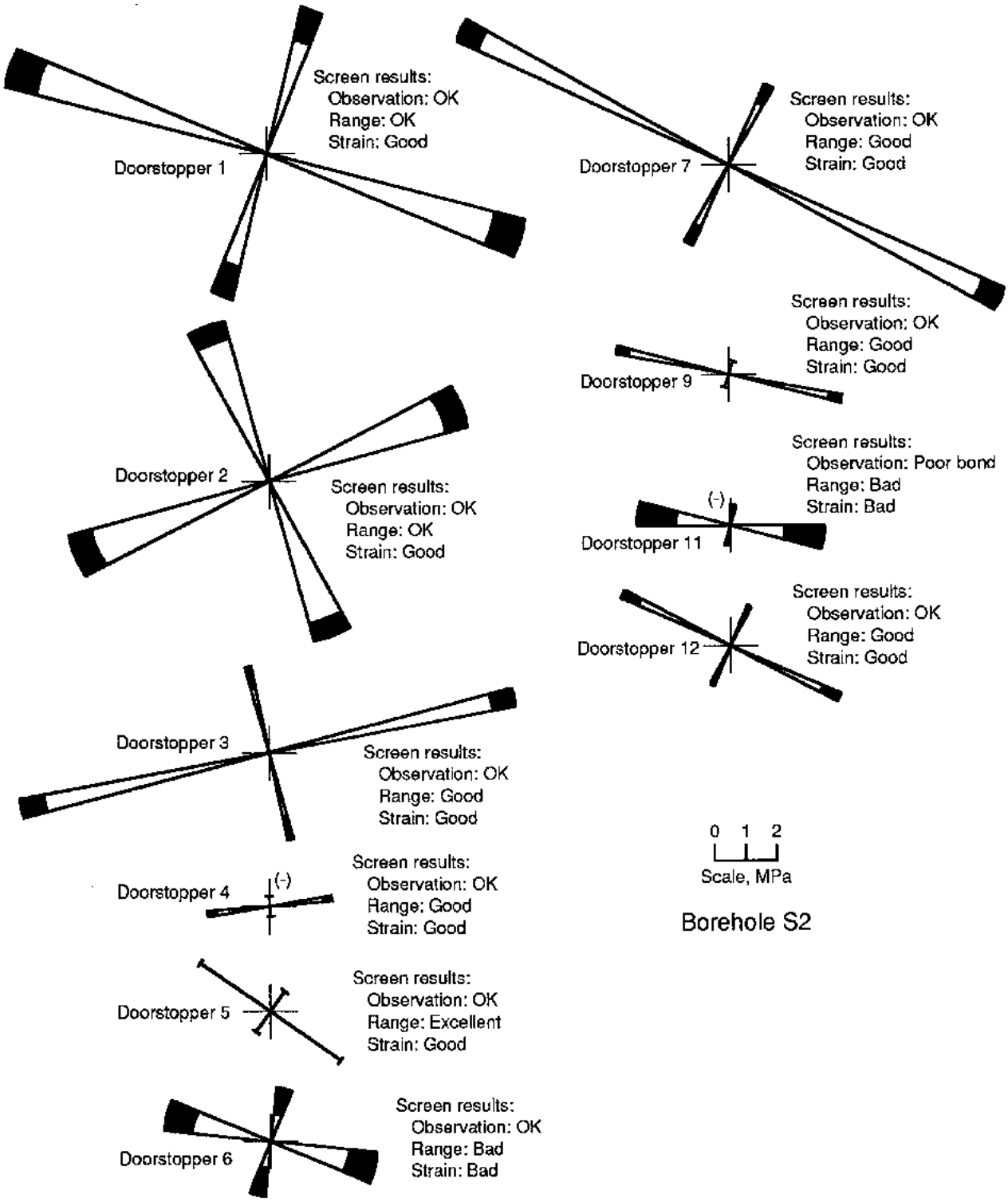

Range of stress fields measured on end of borehole by various sets of strain gauges in each doorstopper cell (see appendix B for calculations). Observations and results of range and strain screens are noted.

Figure 6—Continued

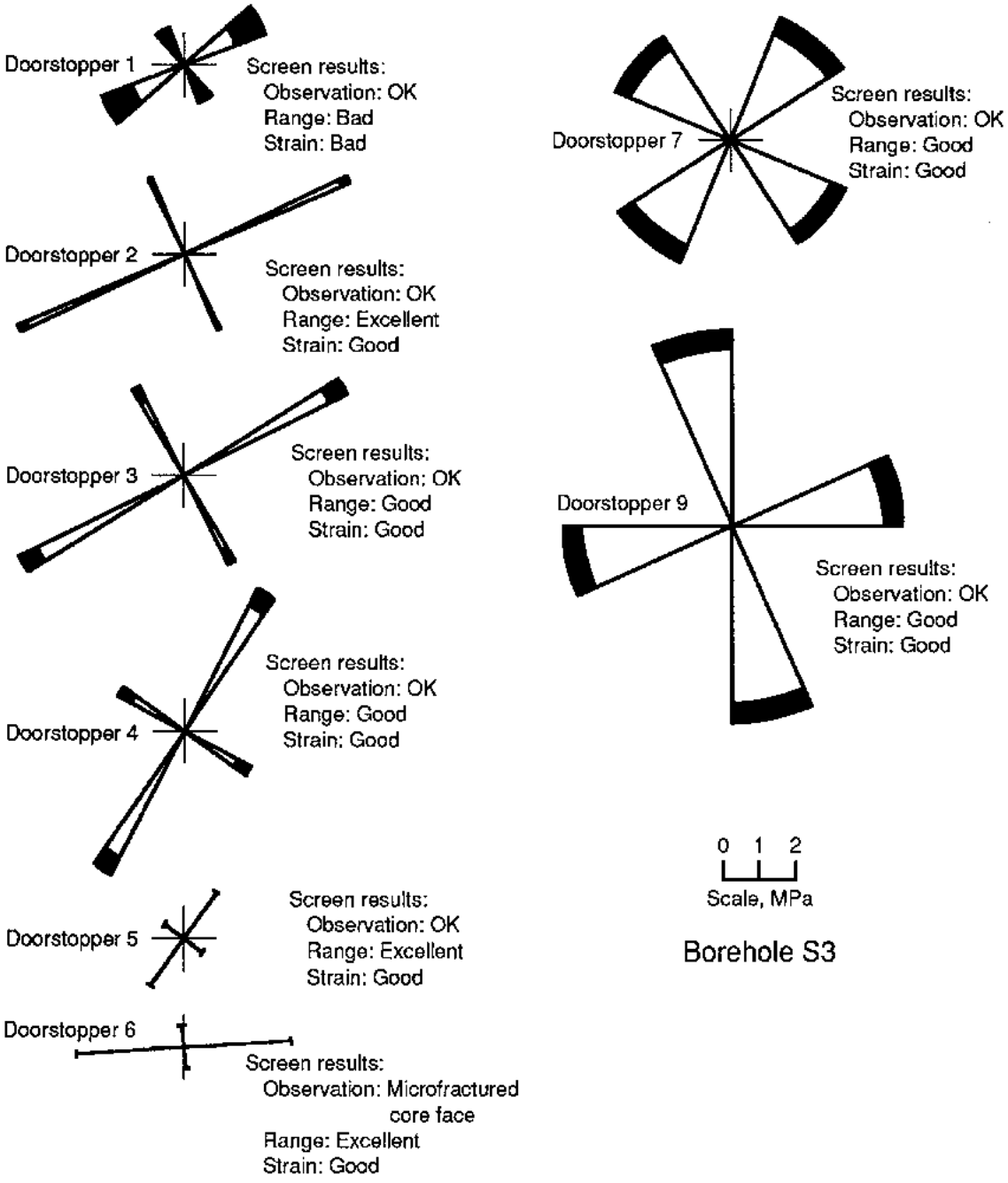

Range of stress fields measured on end of borehole by various sets of strain gauges in each doorstopper cell (see appendix B for calculations). Observations and results of range and strain screens are noted.

Figure 6—Continued

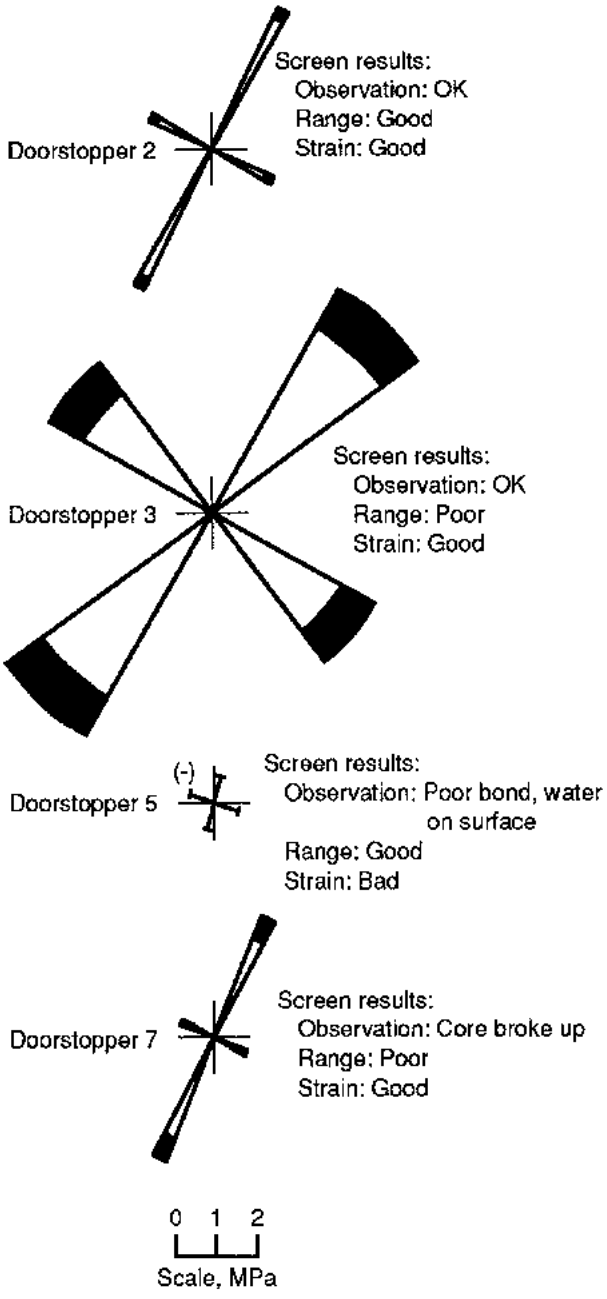

Range of stress fields measured on end of borehole by various sets of strain gauges in each doorstopper cell (see appendix B for calculations). Observations and results of range and strain screens are noted.

test" takes advantage of the fact that any two perpendicular measurements of normal strain define the center of Mohr's circle in strain. Thus, each of two pairs of perpendicular gauges in a doorstopper cell should sum to the same total strain. If the sums are drastically different, the doorstopper cell is failing to measure a single strain field at the end of the borehole. This failure may be attributable to a number of factors, including an electrical fault, the presence of a fracture on or near the face, a poor or nonuniform glue joint, or improper centering of the cell. However, this method will not indicate the source of the strain state, including whether or not isotropic elastic rock is present.

A large difference between the sums for a single cell suggests that the cell should be considered suspect in estimating the in situ stress field. However, defining "large" proved to be problematic. The definition of "large" was chosen arbitrarily as being a difference greater than either 300 με or about 20 pct of the largest sum. This definition was taken from reanalysis of the 4250-level measurement in the first RI (Whyatt and Beus, 1995) of this series, where it proved to be convenient. The strain-screening process and resulting strain-screened data set are summarized in table 7. In this case, all of the cells that failed did so in percentage terms, and a threshold as low as 200 με would not have changed the result.

Table 6.—Range-screen classification by spread of solutions[1]

Doorstopper cell	Percent of variation			Quality[2]
	Orientation	S_1	S_2	
Borehole S1:				
1	0	2	2	Excellent.
2	1	3	3	Excellent.
3	7	29	31	Bad.
4	0	3	3	Excellent.
5	6	19	19	Poor.
6	7	35	33	Bad.
7	8	8	9	Poor.
8	3	12	12	Poor.
9	5	20	10	Bad.
10	23	25	30	Bad.
Borehole S2:				
1	4	11	11	OK.
2	7	7	7	Good.
3	2	8	8	Good.
4	2	10	10	Good.
5	0	1	1	Excellent.
6	9	26	25	Bad.
7	2	8	8	Good.
9	2	9	9	Good.
11	8	37	34	Bad.
12	2	11	11	OK.
13	12	27	30	Bad.
14	6	38	36	Bad.
Borehole S3:				
1	12	32	34	Bad.
2	1	3	3	Excellent.
3	3	9	9	Good.
4	3	9	9	Good.
5	1	3	3	Excellent.
6	1	3	3	Excellent.
7	18	10	8	Good.
9	13	9	10	Good.
Borehole 1-7500:				
1	700	76	68	Bad.
2	2	6	6	Good.
3	14	17	15	Poor.
4	12	68	74	Bad.
5	1	10	10	Good.
7	3	14	14	Poor.

[1]See footnote 5 for explanation of S_1 and S_2.
[2]See appendix C for definition.

Table 7.—Strain screen of data from doorstopper cell overcoring

Doorstopper cell	Summation, με		Difference		Depth, m
	±45°	Horizontal + vertical	με	pct	
7300-LEVEL SITE					
Borehole S1:					
1	549	560	11	2	1.2
2	496	479	42	8	1.3
3	-191	-127	64	34	1.7
4[1]	291	280	11	4	7.2
5[1]	979	834	145	15	7.4
6	-32	-62	30	50	7.7
7[1]	603	565	38	6	7.9
8[1]	500	447	53	12	8.4
9	-182	-225	43	17	11.5
10	980	772	208	21	11.8
Borehole S2:					
1[1]	1,325	1,215	110	8	4.0
2[1]	1,195	1,143	52	4	5.4
3[1]	1,079	1,005	74	7	6.0
4[1]	175	150	25	14	9.1
5[1]	364	368	4	1	9.4
6[1]	404	508	104	20	9.7
7[1]	1,267	1,175	92	7	10.2
9[1]	387	347	40	10	11.0
11	171	301	130	43	11.8
12[1]	584	525	59	10	11.9
13	-51	-39	12	24	12.2
14	32	103	71	69	12.6
Borehole S3:					
1	225	317	92	29	3.4
2[1]	752	734	18	2	3.7
3[1]	753	700	53	7	4.0
4[1]	641	597	44	7	4.3
5[1]	236	230	6	3	4.7
6[1]	342	354	12	3	5.0
7	700	658	42	6	5.3
9	1,006	942	64	6	11.8
7500-LEVEL SITE					
Borehole 1:					
1[1]	2,322	478	1,844	79	2.9
2[1]	558	530	28	5	3.1
3	1,095	967	128	12	5.9
4	-111	132	243	185	6.1
5	28	18	10	36	8.2
7[1]	396	347	49	12	8.7

[1]Doorstopper passed screen test.

The range and strain screens provide generally consistent results (table 8). The exceptions, like doorstopper cells 3 and 9 in borehole S1, are associated with observations that cast doubt on the measurement. A rational screening process could start with elimination of cells where field observations suggested problems, then determination of agreement among the range and strain screens. This combination of screens disqualified four doorstopper cells that appeared to be successful on the basis of field observations. The doorstopper cells that passed the combination of screens are noted in bold italics in table 8.

Table 8.—Comparison of screen results

Doorstopper cell	Strain by gauge orientation, με				Range screen	Strain screen	Notes
	+45°	−45°	Horizontal	Vertical			
					7300-LEVEL SITE		
Borehole S1:							
1	577	−28	619	−59	Excellent	Good	Induced stress zone.
2	363	133	521	−42	Excellent	Good	Induced stress zone.
3	39	−230	−27	−100	Bad	Good	Induced stress zone, bad glue joint, bad surface preparation.
4[1]	24	***267***	***492***	−212	Excellent	Good	
5[1]	275	***704***	***629***	205	Poor	Good	Conglomerate marker bed.
6	46	−78	−7	−55	Bad	Bad	Problem with reading gauges.
7	320	283	210	355	Poor	Good	Crack at center of face.
8[1]	471	29	312	135	Poor	Good	
9	−69	−113	−251	26	Bad	Good	Bad glue joint.
10	525	455	257	515	Bad	Bad	Poor bond, fracture along core.
Borehole S2:							
1[1]	456	***869***	325	***890***	OK	Good	
2[1]	***665***	530	***498***	645	Good	Good	
3[1]	***741***	338	43	***962***	Good	Good	
4[1]	138	***37***	−132	282	Good	Good	
5[1]	−15	379	112	256	Excellent	Good	
6[1]	120	284	118	390	Bad	Bad	
7[1]	114	***1,153***	207	***968***	Good	Good	
9[1]	72	315	−105	452	Good	Good	
11	40	131	−91	392	Bad	Bad	Poor bond.
12[1]	57	527	66	459	OK	Good	
13	−11	−40	−24	−15	Bad	Bad	Poor bond.
14	68	***−36***	−125	228	Bad	Bad	
Borehole S3:							
1	206	19	96	221	Bad	Bad	
2[1]	567	185	204	530	Excellent	Good	
3[1]	573	180	224	476	Good	Good	
4[1]	500	141	395	202	Good	Good	
5[1]	209	27	147	83	Excellent	Good	
6	195	147	−36	390	Excellent	Good	Microfractured core face.
7[1]	382	318	336	322	Good	Good	
9[1]	472	***534***	***533***	409	Good	Good	
					7500-LEVEL SITE		
Borehole 1:							
1	432	1,890	639	−161	Bad	Bad	
2[1]	442	116	371	159	Good	Good	
3[1]	687	408	500	467	Poor	Good	
4	217	−328	178	−46	Bad	Bad	Poor bond, fracture along core.
5	56	−28	123	−105	Good	Bad	Poor bond, water on surface.
7	352	44	301	46	Poor	Good	Core broke up.

[1]Passed observational, range, and strain screens.

NOTE.—Numbers in bold italics indicate a STRESsOUT-screened strain reading.

A widely used screen that is included in the STRESsOUT data-reduction program identifies outlying strains. These are strains that deviate substantially from the average and greatly increase the squared error of the least squares fit estimate of the stress field. The governing assumption in this approach is that outlying data points are attributable to error and not to real conditions. Outlier data can be examined by comparing the results of the range- and strain-screening procedures with the outlier elimination routine in STRESsOUT. In both cases, the field observation screen is applied first. Since the range and strain screens eliminated an additional 4 doorstopper cells with 16 strain readings (about 19 pct of the total remaining 7300-level overcore strains), STRESsOUT was asked to eliminate an equal number of outlying strains, which are identified in table 8. Only one of these, from the −45° gauge of doorstopper 14 in borehole S2, failed to pass the range and strain screens. The lack of overlap between strains eliminated by these two methods suggests that the outlying strains were valid measurements.

7300-LEVEL STRESS FIELD ESTIMATE

Stress estimates were developed with stress concentration factors reported by Rahn (1984) and physical properties reported by Beus and Chan (1980) [i.e., an elastic modulus of 63.8 GPa (9.26 million psi) and a Poisson's ratio of 0.29]. Stress estimates for the full and variously screened data sets gathered at the 7300-level site are presented in table 9.

The original data set produced estimates A and B using the original and current data-reduction procedures, respectively. The difference between these estimates arises from refinements in stress concentration factors, application of a least squares procedure, and recalculation of shear strains. These changes primarily affected the plunge of σ_1 and the magnitudes of the lesser principal stresses.

All of the 7300-level strain measurements were used for developing stress estimate C, a relatively hydrostatic result. Although this unscreened data set contains doorstopper cell measurements corrupted by a wide range of problems, some valid information was probably thrown out in forming the various data sets. For example, the current screen checks to see if all four strain gauges are measuring the same strain field. If only one of the four strain gauges is corrupt, the entire cell, possibly including valid strain information from the other three gauges, is thrown out. These remaining strains might have contributed accurate and vital information that would be lost by screening.

Table 9.—In situ stress estimates from 7300-level data sets passing various screens and reported in situ stress estimate from Beus and Chan (1980)

Stress component	Magnitude		Bearing	Plunge
	GPa	psi		
A. Originally reported stress field estimate:				
σ_1	76	11,000	N 12° W	−28°
σ_2	51	7,400	N 84° W	33°
σ_3	42	6,100	N 54° E	45°
σ_v	50	7,700		
B. Originally selected strains:				
σ_1	81	11,800	N 15° W	13°
σ_2	65	9,400	N 88° E	45°
σ_3	59	8,600	S 63° E	43°
σ_v	63	9,200		
C. All measurements (7300-level site):				
σ_1	44	6,300	N 43° W	6°
σ_2	36	5,300	N 56° E	56°
σ_3	29	4,200	S 42° W	33°
σ_v	34	5,000		
D. Screened for field observations of problems:				
σ_1	50	7,300	N 33° W	11°
σ_2	42	6,000	N 71° E	52°
σ_3	35	5,000	S 49° W	36°
σ_v	40	5,700		
E. Range screen (bad measurements removed):				
σ_1	57	8,200	N 29° W	15°
σ_2	47	6,900	N 84° E	56°
σ_3	38	5,600	S 52° W	30°
σ_v	46	6,600		
F. Range screen (bad and poor measurements removed):				
σ_1	51	7,500	N 14° W	14°
σ_2	42	6,100	N 78° E	61°
σ_3	27	3,900	S 46° W	26°
σ_v	40	5,800		
G. Strain-screened data set:				
σ_1	54	7,800	N 36° W	11°
σ_2	43	6,200	N 76° E	62°
σ_3	33	4,800	S 49° W	25°
σ_v	41	6,000		
H. Measurements included in data sets D, E, and G (best estimate):				
σ_1	54	7,800	N 38° W	10°
σ_2	42	6,000	N 74° E	66°
σ_3	34	4,900	S 48° W	22°
σ_v	41	5,900		
I. Data set D with 16 outlying strains removed:				
σ_1	36	5,200	N 56° W	8°
σ_2	32	4,600	N 47° E	56°
σ_3	14	2,100	S 29° W	33°
σ_v	26	3,800		

NOTE.—Empty cells in columns intentionally left blank.

Field notes on installation problems and other adverse conditions listed in table 8 were used to screen the data set for stress estimate D. The field notes provided the best rational basis for removing overcore strain data, especially in instances where overcore and glue defects were noted. The range and strain screens were used to develop estimates E through G. They resulted in still higher magnitudes and also rotated σ_1 back toward north-northwest. The most thoroughly screened data set, used in estimate K, was formed from strains that survived a combination of field observation, range, and strain screens. This set, containing the common elements of the data sets used to develop estimates D, E, and G, provided a solution that roughly averaged the solution from these latter data sets.

The effect of the screening process as applied both in the original and current analyses was to produce in situ stress field estimates with higher magnitudes of stress, a greater contrast between maximum and minimum stresses, and a rotation of the maximum principal stress direction toward the north. The increased magnitude likely arose from discarding measurements in those instances where the doorstopper gauges did not firmly adhere to the rock.

The final data set (I) was developed from data set D with the outlying 16 strains removed. The independence of the 16 outlying strains from those 16 strains removed by range and strain screening of data set D, noted earlier, resulted in significantly different stress estimates. Removal of good outlying measurements and inclusion of questionable data (by strain- and range-screen standards) cast doubt on this estimate.

These stress estimates can be compared to estimates of gravitational stress and geologic indications of the orientation of tectonic forces. Beus and Chan (1980) estimated overburden stress at 60 MPa (8,670 psi) based on •••••••••• a depth of 2,240 m (7,340 ft) and a rock density of 2,730 kg/m^3 (170 lb/ft^3). This estimate is very close to estimates produced with the original data set, especially after applying the updated analysis process (estimate B in table 9). However, the overburden estimate is probably high as the mine lies under a 460-m (1,500-ft) high hill that is included in the overburden height. A reduced estimate of vertical stress would be more in line with the screened data estimates, but calculation of the topographic influence on overburden stress is deferred to part 4 (Whyatt and others, 1995b) of this series. Most of the stress estimates provide a generally northwest-trending tectonic stress field. This direction agrees with recent movement on the Osburn Fault (Hobbs and others, 1965), which indicates that the maximum stress is horizontal and in the northwest quadrant.

The best stress estimate for the 7300-level site is estimate H in table 9, which follows from the most screened data. This estimate is shown in map coordinates in table 10. The insensitivity of the stress estimates to changes in the screening procedure (except for screening of outlying strains) suggests that the estimate of major stress field characteristics, like orientation of the maximum principal stress, is fairly robust.

Table 10.—Best estimate of stress field in map coordinates

Stress component	Magnitude	
	MPa	psi
σ_{ns}	46	6,700
σ_{ew}	42	6,100
σ_v	41	5,900
$\tau_{ew/ns}$	-9	-1,300
$\tau_{ew/v}$	1	100
$\tau_{ns/v}$	3	500

STRESS FIELD CHARACTERIZATION

The stress field at the measurement site and throughout the mine is fully described by the in situ stress estimate in only the most ideal of cases. That is, the rock mass and stress field are often considerably more complex than the assumptions implicit in the STRESsOUT program's calculations. These assumptions require ideal elastic, homogeneous conditions at each doorstopper cell and across the site as a whole. Often, these conditions are also assumed between sites and throughout the mine. This section attempts to go beyond these assumptions in order to better characterize the stress field.

DOORSTOPPER-SCALE ASSUMPTIONS

The rock immediately surrounding the doorstopper cells was assumed to be homogeneous, continuous, isotropic, and linearly elastic. Uniaxial compression tests showed the rock to be linearly elastic, although some hysterisis at low loads was noted. The available information suggests elastic anisotropy may be a significant factor. However, the scale of the in situ modulus measurements is larger than the scale of the doorstopper cell measurements. The presence of beds of various stiffnesses undoubtedly generates

large-scale orthotropic anisotropy, but it is not clear if there is anisotropy within these beds at the scale of a doorstopper cell overcore as well. Unfortunately, there was insufficient information to determine the thickness of the beds, the proximity of the cells to bed boundaries, or a useful estimate of the degree of anisotropy.

SITE-SCALE ASSUMPTIONS

Assumptions on the scale of a measurement site or sites are particularly important when using two-dimensional cells. These cells are capable only of measuring stress on the face at the end of the borehole. This local stress field has three components, but is determined by four components of the in situ stress field. Thus, the in situ components are underdetermined, and additional information from boreholes in other directions is needed before in situ conditions can be estimated. Data from doorstopper cells in three nonparallel boreholes are needed to estimate the three-dimensional stress state.

The least squares procedure described in the previous section assumes that all doorstopper cells were installed in a homogeneous material experiencing uniform loading. Any deviations from the average of measured material properties or the stress field estimate are considered random errors. The potential for real variability in stress field and/or rock mass properties throughout the measurement site or sites raises two important issues: assessment of stress field variability and the potential for sampling bias. Assessment of stress variability is needed to determine if deviations from ideal conditions are of significant magnitude to influence engineering design, i.e., whether the pattern and/or degree of stress variability can create ground control problems, including rock bursting, if not dealt with explicitly. Furthermore, sampling procedures need to be evaluated in light of any stress field and/or rock property variations to reveal any bias that may exist in estimating average stress conditions.

Local Stress Variability

The degree of local stress variability can be investigated by examining the consistency of similarly oriented overcore measurements. Under ideal conditions, there should be little variability among doorstopper cells installed in a single borehole far from the influence of mine openings. This is rarely the case. Thus, the evaluation process boils down to an investigation of the validity of, and reason for, outlying strain measurements.

Spatial variations in stress can be examined within a borehole, and in the case of parallel boreholes S1 and 1, between boreholes, through the estimates of stress at each doorstopper cell location (figure 6). These solutions, developed for the screening process, are plotted by location in summary plots (figure 7). Large local variations in stress magnitude are evident, even among the best measurements. These local variations overshadow any systematic variation that might exist between boreholes 1 and S1. These local variations may be changes in stress. Alternatively, they may reflect a homogeneous stress field with variations in elastic properties along the boreholes, or some combination of these alternatives. In any case, the assumption of a uniform rock mass under uniform loading is violated.

The degree of variation in stress among the sites might be evident in stress estimates that use borehole 1 (7500- level site) strains to augment or replace borehole S1 (7300-level site) strains used in developing the estimates given in table 9. These estimates are developed in table 11. No adjustments were made to account for the presence of softer argillaceous quartzite observed at the 7500-level site. However, placement of doorstopper cells in zones of good core recovery probably meant that strong, stiff rock was selected at both sites. Unfortunately, more- specific information was not available.

Table 11.—In situ stress estimates from 7300- and 7500-level data sets

Stress component	Magnitude		Bearing	Plunge
	GPa	psi		
A. All measurements, 7300- and 7500-level sites:				
σ_1	44	6,400	N 41° W	7°
σ_2	38	5,500	N 60° E	58°
σ_3	32	4,600	S 45° W	31°
σ_v	36	5,300		
B. All measurements, borehole S1 omitted:				
σ_1	46	6,600	N 36° W	9°
σ_2	41	5,900	N 62° E	41°
σ_3	34	5,000	S 44° W	47°
σ_v	37	5,400		
C. Screened for field observations of problems:				
σ_1	55	8,000	N 14° W	10°
σ_2	47	6,800	N 82° E	31°
σ_3	45	6,600	S 61° W	57°
σ_v	46	6,700		
D. Screened for field observations of problems, borehole S1 omitted:				
σ_1	63	9,200	N 6° E	12°
σ_2	53	7,700	S 82° E	10°
σ_3	49	7,100	S 48° W	74°
σ_v	49	7,200		
E. Screened measurements (data set B after range and strain screens):				
σ_1	58	8,500	N 21° W	20°
σ_2	50	7,300	N 88° E	42°
σ_3	42	6,200	S 50° W	42°
σ_v	48	6,900		

NOTE.—Empty cells in columns intentionally left blank..

Figure 7

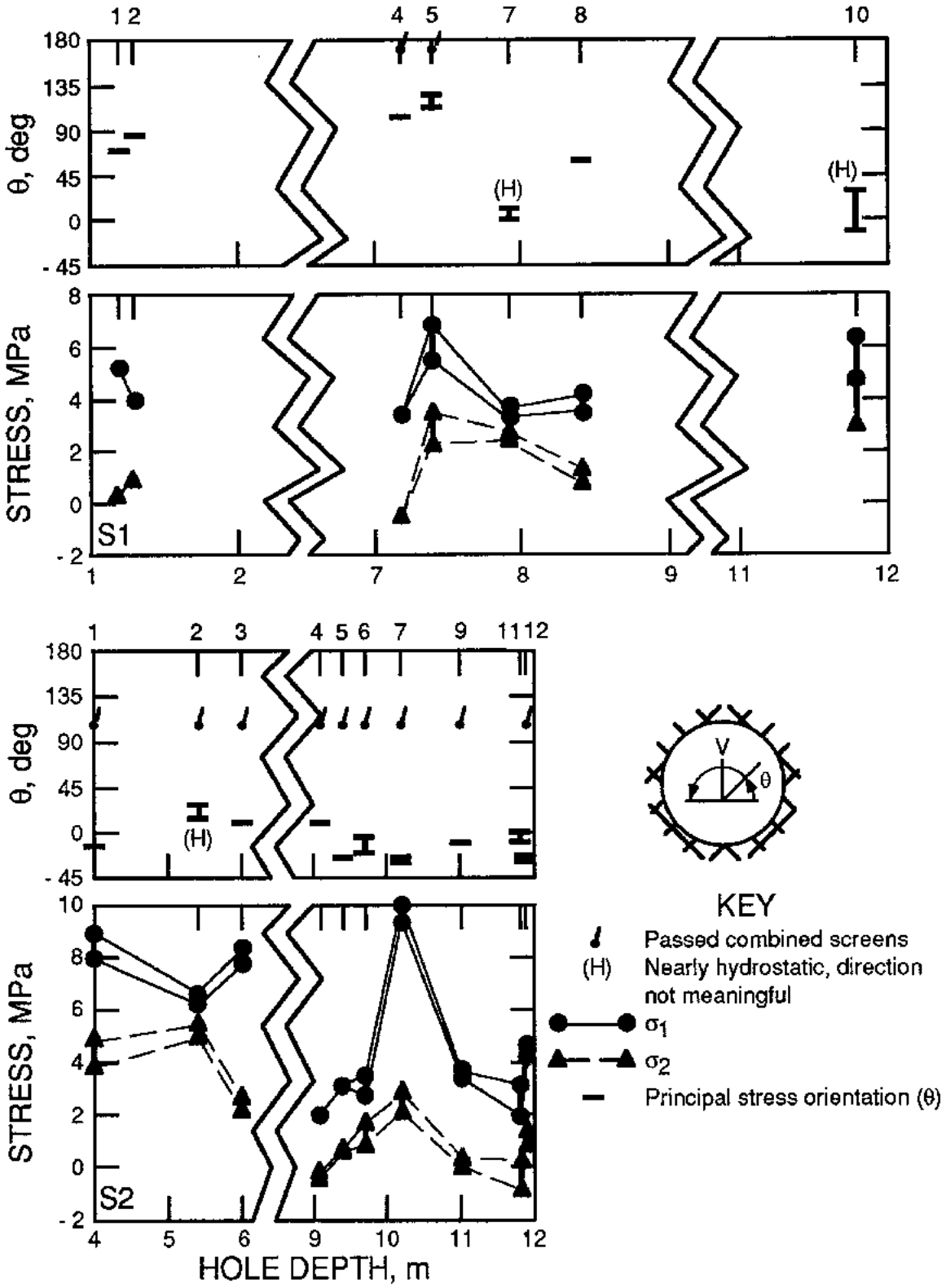

Range of principal stress orientations and magnitudes plotted by relative position in each borehole. Numbers 1 through 12 at the top of the graphs refer to doorstopper cells.

Figure 7—Continued

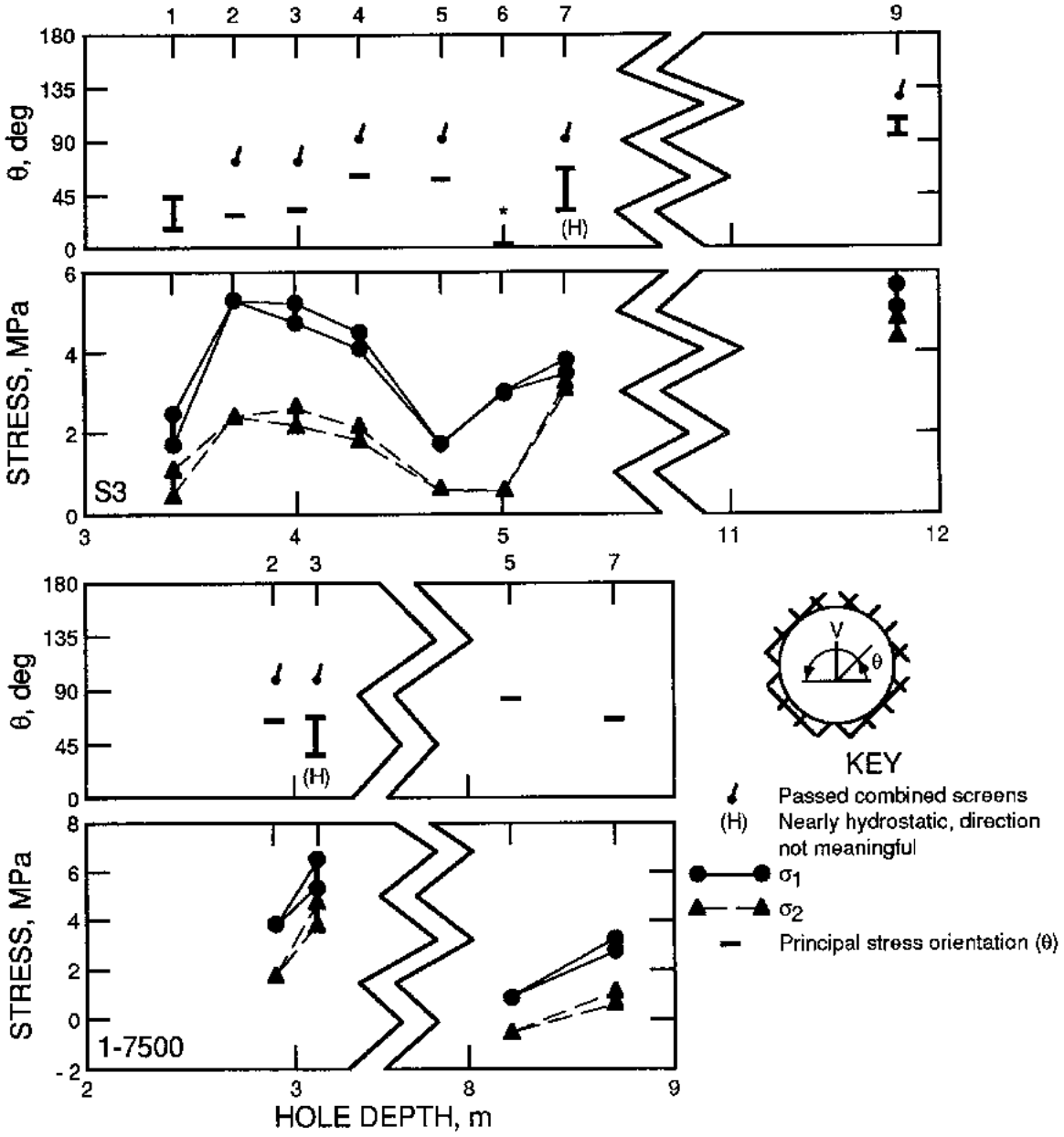

Range of principal stress orientations and magnitudes plotted by relative position in each borehole. Numbers 1 through 12 at the top of the graphs refer to doorstopper cells.

Combining site stress field estimates A, C, and E (table 11), including data from the 7500-level site, causes stress magnitudes to increase and maximum principal stresses to be rotated northward. Omitting borehole S1 strains (estimates B and D) accentuates this trend. The relatively small number of 7500-level measurements that generate this shift (e.g., 6 out of 36 doorstopper cells for the unscreened estimate) suggests that there is a larger difference among sets of overcore strains than was evident from the local stress plots. Moreover, changes in direction and magnitude cannot be explained by changes in depth alone. Because the 7500-level site is north of the Morning East vein in a distinct geologic structure with softer rock and bedding rotated to the north, it would not be surprising to find significantly different overcore strains. The relative influence of changes of rock properties, rotation of orthotropic anisotropy associated with bedding, and/or changes in stress field characteristics cannot be determined from the available data. Thus, this estimate may not describe conditions sampled at the 7500-level site.

It is clear that significant local variations in overcore strains were measured. Moreover, these strains had a significant impact on the stress field estimate. The next logical step in this analysis might be to develop a test site or mine model, as was attempted in part 1 (Whyatt and Beus, 1995) of this series for the 4250-level measurement site. However, there is not enough physical property information to differentiate between variations in overcore strains arising from changes in rock properties and variations reflecting a true change in stress regime.

Sampling

Estimation of a true average stress field for this site is seriously complicated by the presence of real variations in stress and/or rock properties. The spatial distribution of measurements was not a great concern so long as each measurement could be considered an independent, randomly selected data point. But now that spatial dependence of stress and/or material properties has been established, increased attention must be paid to the actual position of the measurement site.

The measurable and unmeasurable sections in each borehole are shown in figure 8. Doorstopper cell core recovery requirements disqualified a large portion of each borehole. For example, 10 measurements in borehole 1 were concentrated in 3 sections composing only 3 m (6 ft) of the available 12 m (36 ft). Whether poor core recovery was a result of preexisting fractures, core discing, or drilling is unclear. The unmeasured sections probably represent zones of relatively weak, soft rock with relatively lower levels of stress, while the measured portions were probably selectively positioned inside thicker beds. Thus, this measurement was likely biased by concentrated sampling. Unfortunately, there is insufficient information available to evaluate the degree of bias.

Figure 8

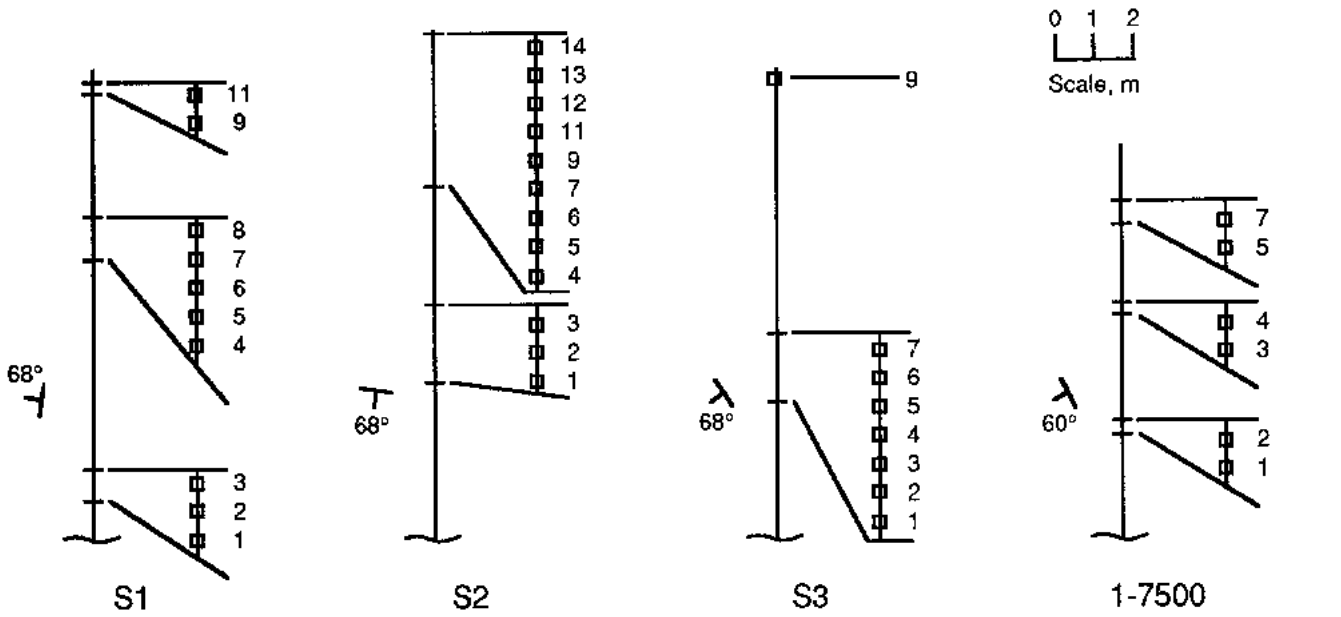

Location of doorstopper cells and orientation of bedding for each overcore measurement borehole.

DISCUSSION AND CONCLUSIONS

The estimated in situ stress field deep in the Star Mine was updated by applying contemporary data-reduction procedures and systematic data-screening methods to overcore stress measurements reported by Beus and Chan (1980). The estimated stress was reduced in magnitude and rotated toward the northwest by the new procedure, which resulted in the estimates shown in table 12.

Table 12.—Best estimate of average stress state at 7300-level measurement site

Stress component	Magnitude		Bearing	Plunge
	GPa	psi		
σ_1	54	7,800	N 38° W	10°
σ_2	42	6,000	N 74° E	66°
σ_3	34	4,900	S 48° W	22°
σ_v	41	5,900		

NOTE.—Empty cells in columns intentionally left blank.

The direction of σ_1 in this estimate is more in line with tectonic evidence of a northwest stress field than the direction indicated in the original analysis by Beus and Chan (1980). The vertical stress estimate is lower than the previous estimate and lower than simple overburden calculations would suggest, but the measurement site is located under a hill, and as the 5300-level measurement investigated in part 2 (Whyatt and others, 1995a) demonstrated, equilibrium can only be used to estimate average overburden stress. In situ tests conducted at the site suggested significant anisotropy at comparatively large scales (a meter or two). There was no indication of the degree of doorstopper-scale anisotropy, and this factor was not considered in either the estimate of Beus and Chan or the current estimate.

Inspection and screening of individual doorstopper cell measurements revealed that there was considerable variability among cells, even cells mounted within a fraction of a meter of each other in the same borehole. Furthermore, sets of outlier strains were almost completely independent of one another, and these contributed most significantly to the measurements of squared error and sets of questionable strains identified by other means. This independence demonstrates that the variability was real and could not be attributed to measurement error. The admission that local overcore strain variability exists violates many of the assumptions underlying contemporary stress estimation procedures and introduces the question of sampling bias. Unfortunately, there is insufficient geologic and rock property information to address these issues. If more information were available, alternative models of stress site conditions could be proposed, as was done for the Lucky Friday 4250-level analysis described in part 1 (Whyatt and Beus, 1995) of this series.

While this analysis improved the stress field estimate, it also highlighted the sources of uncertainty that plague overcore measurements in complex geologic settings. Moreover, it served to underscore the importance of treating an overcore stress measurement as a geomechanical experiment investigating the geologic structure and stress patterns at a site. If an estimate of average far-field stresses is sought, a priori investigation of possible stress contorting geologic structures is appropriate. The change in rock type across the Morning East vein and the intersection of veins near the 7300- and 7500-level sites are probably representative of stress-contorting structures. Site investigations and stress measurement studies need to include comprehensive rock testing programs that evaluate stress estimation assumptions as well as supply the required elastic properties.

Finally, mines containing complex geologic structures cannot be considered to lie in homogeneous stress fields. Rock-burst experience at the 5300-level site discussed in part 2 (Whyatt and others, 1995a) demonstrates that variations in the stress field may have significant ground control implications. Obviously, mine-scale stress variations cannot be measured by overcore methods alone. However, stress characteristics are often revealed in the course of normal mine exploration drilling and the excavation of normal mine openings. The final report of this series examines nonovercore evidence of stress field characteristics at the Lucky Friday Mine and attempts to discover how the in situ stress field varies throughout the host geologic structure.

A favored or "best guess" estimate of the stress field at the Star Mine can be derived in two different ways. The first, used in the original analysis of these data, considers other evidence of stress field characteristics and looks for consistency as an indicator of measurement quality. The second, applied in the screening process presented here, includes a test to eliminate prejudgment of results in favor of decisions based on self-consistency of instrument readings. Both approaches incorporate field observations of instrument operation.

The choice depends primarily on understanding the possible stress field characteristics at a measurement site. With the tremendous increase in the number of in situ stress studies that have become available in the 15 years since this measurement was made, it has become increasingly clear that local deviations in the stress field are common and may include substantial residual and structural stresses. Thus, confidence in estimates of what a stress field "ought to be" has been significantly eroded, and the best policy is to avoid biasing the result with expectations.

The screened data set with the 7500-level site data removed was judged to provide the best estimate of the in situ stress field (estimate F in table 9). The reasons for this judgment include the rational and consistent screening of data and the elimination of measurements from a potentially different stress field at the 7500-level site.

REFERENCES

Amadei, B., and W. Z. Savage. Determination of the Elastic Properties of Anisotropic Rock Masses From In-Situ Expansion Tests. Paper in Rock Mechanics as a Multidisciplinary Science: Proceedings of the 32nd U.S. Symposium, ed. by J.-C. Roegiers (Univ. OK, Norman, OK, July 10-12, 1991). Balkema, 1991, pp. 303-312.

Beus, M. J., and S. S. M. Chan. Shaft Design in the Coeur d'Alene Mining District—Results of In Situ Stress and Physical Property Measurements. USBM RI 8435, 1980, 39 pp.

Bonnechere, F. A., and C. Fairhurst. Determination of Regional Stress Field From "Doorstopper" Measurements. Paper in International Symposium on the Determination of Stresses in Rock Masses (Proc., Lisbon, Portugal, 1969). Natl. Lab. Civil Eng., Lisbon, Portugal, 1971, pp. 307-333.

Dalley, J. W., and W. F. Riley. Experimental Stress Analysis. McGraw-Hill, 2nd ed., 1978, pp. 318-333.

Goodman, R. E. Introduction to Rock Mechanics. John Wiley, 1980, pp. 121-123.

Hobbs, S. W., A. B. Griggs, R. E. Wallace, and A. B. Campbell. Geology of the Coeur d'Alene District, Shoshone County, Idaho. U.S. Geol. Surv. Prof. Pap. 478, 1965, 139 pp.

Hocking, G. Three-Dimensional Elastic Stress Distribution Around the Flat End of a Cylindrical Cavity. Int. J. Rock Mech. Min. Sci. Geomech. Abstr., v. 13, No. 12, 1976, pp. 331-337.

Hustrulid, W. Development of a Borehole Device To Determine the Modulus of Rigidity of Coal Measure Rocks. USBM OFR 12-72, 1971, 119 pp.; NTIS PB 209 548/AS.

International Society for Rock Mechanics. Suggested Methods for Rock Stress Determination. Int. J. Rock Mech. Min. Sci. Geomech. Abstr., v. 24, No. 1, 1987, pp. 53-74.

Jenkins, M., and R. McKibbin. Practical Considerations of In Situ Stress Determination. Ch. in Proceedings, International Symposium on Application of Rock Characterization Techniques in Mine Design, ed. by M. Karmis. Soc. Min. Eng., 1986, pp. 33-39.

Larson, M. K. STRESsOUT—A Data Reduction Program for Inferring Stress State of Rock Having Isotropic Material Properties: A User's Manual. USBM IC 9302, 1992, 163 pp.

Patricio, J. G., and M. J. Beus. Determination of the In Situ Modulus of Deformation in Hard Rock Mines of the Coeur d'Alene District, Idaho. Paper in Site Characterization, 17th Symposium on Rock Mechanics (Salt Lake City, UT). UT Eng. Exper. Stat., Univ. UT, Salt Lake City, UT, 1976, pp. 4B9-1 to 4B9-7.

Rahn, W. Stress Concentration Factor for the Interpolation of "Doorstopper" Stress Measurements in Anisotropic Rocks. Int. J. Rock Mech. Min. Sci. Geomech. Abstr., v. 21, No. 6, 1984, pp. 313-326.

Van Heerden, E. W. Stress Concentration Factors for the Flat Borehole End for Use in Rock Stress Measurements. Eng. Geol., v. 3, 1969, pp. 307-323.

Whyatt, J. K. Geomechanics of the Caladay Shaft. M.S. Thesis, Univ. ID, Moscow, ID, 1986, 195 pp.

Whyatt, J. K., and M. J. Beus. In Situ Stress at the Lucky Friday Mine (In Four Parts): 1. Reanalysis of Overcore Measurements From 4250 Level. USBM RI 9532, 1995, 26 pp.

Whyatt, J. K., F. M. Jenkins, and M. K. Larson. In Situ Stress at the Lucky Friday Mine (In Four Parts): 2. Analysis of Overcore Measurement From 5300 Level. USBM RI 9560, 1995a.

Whyatt, J. K., T. J. Williams, and W. Blake. In Situ Stress at the Lucky Friday Mine (In Four Parts): 4. Characterization of Mine In Situ Stress Field. USBM RI, 1995b, in press.

APPENDIX A.—SENSITIVITY OF STRESS FIELD ESTIMATE TO CHOICE OF STRESS CONCENTRATION FACTOR

The influence of the updated data-reduction process in STRESsOUT and application of better concentration factors proposed by a number of researchers (Bonnechere and Fairhurst, 1971; Hocking, 1976; Rahn, 1984; Van Heerden, 1969) are explored in table A-1. All of these calculations proceed from the original six strain measurements, correctly interpreted, that were used in the original solution. A very large contrast is evident between the originally reported stress estimate and an estimate derived using the original stress concentration factors and the STRESsOUT program. A similar but opposite shift is evident as updated stress concentration factors are applied. Thus, it appears that the problems with strain misdefinition and poor stress concentration factors were compensating conditions, resulting in a surprisingly good estimate of in situ stress.

Table A-1.—Stress solutions based on original six composite strain measurements

Stress component	Magnitude		Bearing	Plunge
	GPa	psi		
A. Originally reported stress field:				
σ_1	76	11,000	N 12° W	-28°
σ_2	51	7,400	N 84° W	33°
σ_3	42	6,100	N 54° E	45°
σ_v	50	7,300		
B. Original stress concentration factors, where a = 1.25, b = 0, c = 0, and d = 1.25 (Chan and Beus, see footnote 2 in main text):[1]				
σ_1	51	7,300	N 18° W	12°
σ_2	25	3,700	S 79° E	66°
σ_3	20	2,900	S 68° W	21°
σ_v	26	3,800		
C. Factors reported by Bonnechere and Fairhurst (1971), where a = 1.25, b = 0, c = -0.51, and d = 1.25:[1]				
σ_1	74	10,700	N 17° W	18°
σ_2	52	7,500	S 88° E	45°
σ_3	47	6,800	S 58° W	39°
σ_v	52	7,500		
D. Factors developed for Poisson's ratio = 0.18 (after Van Heerden, 1969), where a = 1.36, b = -0.03, c = -0.69, and d = 1.39:[1]				
σ_1	81	11,700	N 16° W	19°
σ_2	61	8,900	S 89° E	43°
σ_3	57	8,300	S 56° W	42°
σ_v	61	8,900		
E. Factors developed according to equations reported by Rahn (1984), where a = 1.34, b = -0.03, c = -0.68, and d = 1.38:[1]				
σ_1	81	11,800	N 16° W	19°
σ_2	61	8,900	S 88° E	43°
σ_3	57	8,200	S 56° W	42°
σ_v	61	8,900		

[1]Stress concentration factors are used in equations 2, 3, and 4 in the main text.

NOTE,—Empty cells in columns intentionally left blank.

APPENDIX B.—DOORSTOPPER CELL LOCAL SOLUTIONS

The strain field at the *end* of a borehole can be estimated from doorstopper cell strain readings (e.g., equation 1). By using Hooke's law, the stress on the end of the borehole can be determined easily [see Goodman (1980) for a more complete treatment]. The solutions for each doorstopper are presented in table B-1, and the ranges are summarized in table B-2. These solutions are illustrated in figure 6 and summarized in figure 7. These figures show the range of stress solutions that follow from solutions using various combinations of three of the four doorstopper cell strain gauges. These estimates were developed for a rock modulus of 63.8 GPa (9.26 million psi) and a Poisson's ratio of 0.29.

Table B-1.—Stress solutions for end of borehole using various combinations of three strain gauges at each doorstopper cell location[1]

Stress attributes	Solution 1	Solution 2	Solution 3	Solution 4
BOREHOLE S1				
Doorstopper 1:				
Θ, deg	69	69	69	69
S_1, MPa	5.13	5.12	5.17	5.07
S_2, MPa	0.31	0.22	0.27	0.26
Doorstopper 2:				
Θ, deg	78	79	80	79
S_1, MPa	3.97	3.99	3.94	4.08
S_2, MPa	0.68	0.83	0.72	0.74
Doorstopper 3:				
Θ, deg	55	58	51	46
S_1, MPa	-0.04	-0.12	0.29	-0.21
S_2, MPa	-1.20	-1.73	-1.53	-1.65
Doorstopper 4:				
Θ, deg	99	100	100	99
S_1, MPa	3.34	3.38	3.36	3.43
S_2, MPa	-0.62	-0.55	-0.64	-0.61
Doorstopper 5:				
Θ, deg	107	118	117	109
S_1, MPa	5.41	6.12	5.96	6.66
S_2, MPa	2.69	3.39	2.14	2.85
Doorstopper 6:				
Θ, deg	54	49	59	61
S_1, MPa	0.13	0.18	-0.02	0.24
S_2, MPa	-0.73	-0.49	-0.58	-0.55
Doorstopper 7:				
Θ, deg	14	6	0	10
S_1, MPa	3.18	3.43	3.13	3.23
S_2, MPa	2.31	2.43	2.36	2.63
Doorstopper 8:				
Θ, deg	55	53	57	59
S_1, MPa	3.58	3.66	3.31	3.76
S_2, MPa	0.77	1.20	1.03	1.10
Doorstopper 9:				
Θ, deg	9	4	0	5
S_1, MPa	-0.32	-0.02	-0.35	-0.25
S_2, MPa	-1.87	-1.75	-1.83	-1.52
Doorstopper 10:				
Θ, deg	24	4	-14	27
S_1, MPa	4.76	6.02	4.53	4.99
S_2, MPa	2.74	3.50	2.97	4.5
BOREHOLE S2				
Doorstopper 1:				
Θ, deg	-14	-16	-21	-21
S_1, MPa	7.61	8.55	7.96	8.08
S_2, MPa	4.19	4.32	3.84	4.79

See footnote at end of table.

Table B-1.—Stress solutions for end of borehole using various combinations of three strain gauges at each doorstopper cell location[1]—Continued

Stress attributes	Solution 1	Solution 2	Solution 3	Solution 4
BOREHOLE S2—Continued				

Doorstopper 2:				
Θ, deg	26	17	15	27
S_1, MPa	6.19	6.45	6.00	6.25
S_2, MPa	4.92	5.16	5.10	5.36
Doorstopper 3:				
Θ, deg	14	11	10	13
S_1, MPa	7.65	8.11	7.49	7.74
S_2, MPa	2.11	2.30	2.27	2.74
Doorstopper 4:				
Θ, deg	8	6	5	7
S_1, MPa	1.89	2.05	1.85	1.92
S_2, MPa	−0.43	−0.35	−0.40	−0.22
Doorstopper 5:				
Θ, deg	−35	−35	−35	−35
S_1, MPa	2.92	2.89	2.90	2.89
S_2, MPa	0.66	0.65	0.68	0.64
Doorstopper 6:				
Θ, deg	−22	−22	−6	−12
S_1, MPa	3.49	2.59	3.21	3.06
S_2, MPa	1.45	1.33	1.72	0.87
Doorstopper 7:				
Θ, deg	−26	−25	−28	−29
S_1, MPa	8.95	9.75	9.35	9.46
S_2, MPa	2.46	2.56	2.06	2.85
Doorstopper 9:				
Θ, deg	−10	−11	−13	−13
S_1, MPa	3.27	3.60	3.36	3.41
S_2, MPa	0.10	0.16	0.02	0.35
Doorstopper 11:				
Θ, deg	−12	−7	2	−4
S_1, MPa	2.88	1.80	2.76	2.49
S_2, MPa	0.04	−0.14	0.17	−0.83
Doorstopper 12:				
Θ, deg	−23	−23	−27	−27
S_1, MPa	4.07	4.58	4.31	4.38
S_2, MPa	1.03	1.09	0.79	1.30
Doorstopper 13:				
Θ, deg	31	48	39	27
S_1, MPa	−0.14	−0.17	−0.08	−0.15
S_2, MPa	−0.24	−0.33	−0.30	−0.34
Doorstopper 14:				
Θ, deg	3	10	13	7
S_1, MPa	1.45	0.96	1.55	1.32
S_2, MPa	−0.45	−0.65	−0.55	−1.01
BOREHOLE S3				
Doorstopper 1:				
Θ, deg	19	40	33	20
S_1, MPa	1.96	1.60	2.36	1.86
S_2, MPa	1.12	0.59	0.72	0.33
Doorstopper 2:				
Θ, deg	25	24	24	26
S_1, MPa	4.94	5.03	4.87	4.96
S_2, MPa	2.19	2.28	2.26	2.34
Doorstopper 3:				
Θ, deg	30	26	27	32
S_1, MPa	4.77	4.99	4.53	4.83
S_2, MPa	2.03	2.33	2.27	2.48

See footnote at end of table.

Table B-1.—Stress solutions for end of borehole using various combinations of three strain gauges at each doorstopper cell location[1]—Continued

Stress attributes	Solution 1	Solution 2	Solution 3	Solution 4
	BOREHOLE S3—Continued			
Doorstopper 4:				
Θ, deg	58	56	61	62
S_1, MPa	4.09	4.15	3.89	4.26
S_2, MPa	1.71	2.07	1.91	1.96
Doorstopper 5:				
Θ, deg	54	54	55	56
S_1, MPa	1.65	1.66	1.62	1.67
S_2, MPa	0.59	0.64	0.62	0.62
Doorstopper 6:				
Θ, deg	2	3	4	3
S_1, MPa	2.86	2.78	2.87	2.84
S_2, MPa	0.58	0.55	0.57	0.48
Doorstopper 7:				
Θ, deg	49	33	61	66
S_1, MPa	3.48	3.59	3.27	3.63
S_2, MPa	2.91	3.21	3.13	3.17
Doorstopper 9:				
Θ, deg	90	113	113	99
S_1, MPa	4.91	5.12	5.05	5.42
S_2, MPa	4.24	4.66	4.10	4.36
	BOREHOLE 1-7500			
Doorstopper 1:				
Θ, deg	77	153	128	104
S_1, MPa	4.70	16.07	11.40	19.35
S_2, MPa	−0.05	6.48	−6.76	3.21
Doorstopper 2:				
Θ, deg	60	60	63	63
S_1, MPa	3.68	3.71	3.55	3.79
S_2, MPa	1.47	1.71	1.60	1.63
Doorstopper 3:				
Θ, deg	47	36	51	60
S_1, MPa	5.79	6.11	5.11	6.18
S_2, MPa	3.60	4.53	4.28	4.46
Doorstopper 4:				
Θ, deg	63	65	53	44
S_1, MPa	1.65	1.38	2.83	0.92
S_2, MPa	−0.36	−2.46	−1.55	−2.00
Doorstopper 5:				
Θ, deg	79	79	81	80
S_1, MPa	0.75	0.76	0.73	0.81
S_2, MPa	−0.57	−0.49	−0.55	−0.54
Doorstopper 7:				
Θ, deg	63	62	67	67
S_1, MPa	2.86	2.91	2.66	3.08
S_2, MPa	0.51	0.93	0.71	0.77

See footnote 5 in main text for explanation of S_1 and S_2.

Table B-2.—Range of individual doorstopper cell solutions for stress on end of borehole[1]

Doorstopper cell	Orientation of S_1, deg		S_1, MPa		S_2, MPa	
	Minimum	Maximum	Minimum	Maximum	Minimum	Maximum
Borehole S1:						
1	69	69	5.07	5.17	0.22	0.31
2	78	80	3.94	4.08	0.68	0.83
3	46	48	-0.21	0.29	-1.73	-1.20
4	99	100	3.34	3.43	-0.64	-0.55
5	107	118	5.41	6.66	2.14	3.39
6	49	61	-0.02	0.24	-0.73	-0.49
7	0	14	3.13	3.43	2.31	2.63
8	53	59	3.31	3.76	0.77	1.20
9	0	9	-0.35	-0.02	-1.87	-1.52
10	-14	27	4.53	6.02	2.74	4.50
Borehole S2:						
1	-21	-14	7.61	8.55	3.84	4.79
2	15	27	6.00	6.45	4.92	5.36
3	10	14	7.49	8.11	2.11	2.74
4	5	8	1.85	2.05	-0.43	-0.22
5	-35	-35	2.89	2.92	0.64	0.68
6	-22	-6	2.59	3.49	0.87	1.72
7	-29	-25	8.95	9.75	2.06	2.85
9	-13	-10	3.27	3.60	0.02	0.35
11	-12	2	1.80	2.88	-0.83	0.17
12	-27	-23	4.07	4.58	0.79	1.30
13	27	48	-0.17	-0.08	-0.34	-0.24
14	3	13	0.96	1.55	-1.01	-0.45
Borehole S3:						
1	19	40	1.60	2.36	0.33	1.12
2	24	26	4.87	5.03	2.19	2.34
3	26	32	4.53	4.99	2.03	2.48
4	56	62	3.89	4.26	1.71	2.07
5	54	56	1.62	1.67	0.59	0.64
6	2	4	2.78	2.87	0.48	0.58
7	33	66	3.27	3.63	2.91	3.21
9	90	113	4.91	5.42	4.10	4.66
Borehole 1-7500:						
1	77	153	4.70	19.35	-6.76	6.48
2	60	63	3.55	3.79	1.47	1.71
3	36	60	5.11	6.18	3.60	4.53
4	44	65	0.92	2.83	-2.46	-0.36
5	79	81	0.73	0.81	-0.57	-0.49
7	62	67	2.66	3.08	0.51	0.93

[1]See footnote 5 in main text for explanation of S_1 and S_2.

APPENDIX C.—RANKING CRITERIA FOR QUALITY DESIGNATION[1]

Quality	Maximum percent of variation		
	Orientation[2]	[3]S_1	[4]S_2
Excellent	1	5	5
Good	3	10	10
Acceptable	5	15	15
Poor	10	20	20
Bad	>30	>20	>20

[2][1]See text footnote 5 in main text for explanation of S_1 and S_2.

$$\frac{\Theta_{max} - \Theta_{min}}{180^\circ} \times 100.$$

[3] $$\frac{S_{1\text{-}max} - S_{1\text{-}min}}{S_{1\text{-}max}} \times 100.$$

[4] $$\frac{S_{2\text{-}max} - S_{2\text{-}min}}{S_{1\text{-}max}} \times 100.$$